An eikonal based formulation for traveltime perturbation with respect to the source location[a]

[a]Published in Geophysics, 75, T175-T183 (2010)

Tariq Alkhalifah and Sergey Fomel[1]

ABSTRACT

Traveltime calculations amount to solving the nonlinear eikonal equation for a given source location. We analyze the relationship between the eikonal solution and its perturbations with respect to the source location and develop a partial differential equation that relates the traveltime field for one source location to that for a nearby source. This linear first-order equation in one form depends on lateral changes in velocity and in another form is independent of the velocity field and relies on second-order derivatives of the original traveltime field. For stable finite-difference calculations, this requires the velocity field to be smooth in a sense similar to ray-tracing requirements. Our formulation for traveltime perturbation formulation has several potential applications, such that fast traveltime calculation by source-location perturbation, velocity-independent interpolation including datuming, and velocity estimation. Additionally, higher-order expansions provide parameters necessary for Gaussian-beam computations.

INTRODUCTION

The traveltime field is typically used to describe the phase behavior of the Green's function, a key tool for Kirchhoff modeling and migration. It also is used at the heart of many velocity estimation applications, such as reflection tomography. The traveltime field for a fixed source in a heterogeneous medium is governed by the eikonal equation, derived about 150 years ago by Sir William Rowan Hamilton. Since early 1990s, a direct numerical solution of the eikonal equation has been a popular method of computing traveltimes on regular grids, commonly used in seismic imaging (Vidale, 1988, 1990; van Trier and Symes, 1991; Podvin and Lecomte, 1991). Modern methods of traveltime computation include the *fast marching* method, developed by Sethian (1996) in the general context of level set methods for propagating interfaces. Sethian and Popovici (1999) and Popovici and Sethian (2002) report a successful application of this method in three-dimensional seismic computations. Alkhalifah and Fomel (2001) improved its accuracy using spherical coordinates. Alternative methods include group fast marching (Kim, 2002), fast sweeping (Zhao, 2005), and

[1]**e-mail:** tkhalfah@kacst.edu.sa, sergey@sep.stanford.edu

paraxial marching (Qian and Symes, 2002). Several alternative schemes are reviewed by Kim (2002).

The nonlinear nature of the eikonal partial differential equation was addressed by Aldridge (1994), who linearized the eikonal equation with respect to velocity perturbation, while retaining its first-order nature. Alkhalifah (2002) developed a similar linearization formula for perturbations in anisotropic parameters and solved it numerically using the fast marching method. The linear feature increased the efficiency and stability of the numerical solution, especially in the anisotropic case.

A major drawback of using conventional methods to solve the eikonal equation numerically is that we only evaluate the fastest arrival solution, not necessarily the most energetic one. This results in less than acceptable traveltime computation for imaging in complex media (Geoltrain and Brac, 1993). Eikonal solvers can be extended to image multiple arrivals through semi-recursive Kirchhoff migration (Bevc, 1997), phase-space equations (Fomel and Sethian, 2002), or slowness matching (Symes and Qian, 2003) techniques. The linearization also helps to avoid the first-arrival only limitation, especially when the background traveltime field includes energetic arrivals.

The dependence of the traveltime field on the source location can be empirically evaluated by comparing the shape of the traveltime fields for two different sources when the sources are superimposed on each other. For a medium with no lateral velocity variation, the traveltime field should be source-location independent. Relating the two traveltime fields directly through an equation can provide insights into the dependence of traveltime fields on lateral velocity variations. Such information can serve in developing better traveltime interpolation and velocity estimation.

In this paper, we develop a new eikonal-based partial differential equation that relates traveltime shape changes to changes in the source location. The changes can be described first- or second-order accurate terms and thus used in a Taylor's type expansion to find the traveltime for a nearby source. We test the accuracy of the approximation analytically and numerically through the use of complex synthetic models. In the discussion section, we suggest possible applications for the new equation.

SHIFT IN THE SOURCE LOCATION

The eikonal equation appears in the zeroth-order asymptotic expansion of the solution of the wave equation given by the Wentzel, Kramers, and Brillouin (WKB) approximation. It represents the geometrical optics term that contains the most rapidly varying component of the leading behavior of the expansion. In a medium with sloth (slowness squared), w, the traveltime τ for a wavefield emanating from a source satisfies the following formula:

$$\left(\frac{\partial \tau}{\partial x}\right)^2 + \left(\frac{\partial \tau}{\partial y}\right)^2 + \left(\frac{\partial \tau}{\partial z}\right)^2 = w(x,y,z), \tag{1}$$

where (x, y, z) are the components of the 3-D medium. At the location of the source (x_s, y_s, z_s), the initial value of time $\tau(x_s, y_s, z_s) = 0$ is needed for numerically solving the eikonal equation 1. Moving the source along the x-axis a distance l is equivalent to solving the following eikonal equation:

$$\left(\frac{\partial \tau}{\partial x}\right)^2 + \left(\frac{\partial \tau}{\partial y}\right)^2 + \left(\frac{\partial \tau}{\partial z}\right)^2 = w(x - l, y, z), \tag{2}$$

for the same source location. In other words, we are replacing a shift in the source location with an equal distance shift in the velocity field in the opposite direction. Figure 1 shows the operation for a single source and image point combination taking into account the reciprocity principle between sources and receivers.

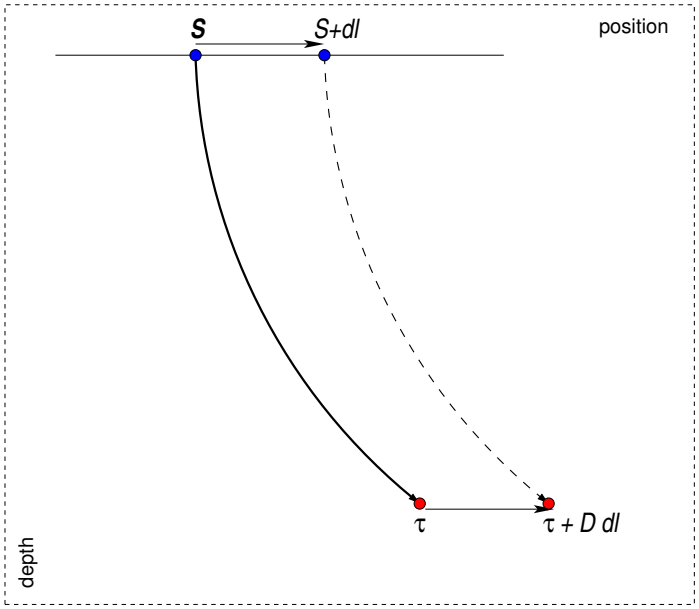

Figure 1: Illustration of the relation between the initial source location and a perturbed version given by a single source and image point locations. This is equivalent to a shift in the velocity field laterally by dl.

Assuming that the sloth (or velocity) field is continuous in the x direction, we differentiate equation 2 with respect to l and get:

$$2\frac{\partial \tau}{\partial x}\frac{\partial^2 \tau}{\partial x \partial l} + 2\frac{\partial \tau}{\partial y}\frac{\partial^2 \tau}{\partial y \partial l} + 2\frac{\partial \tau}{\partial z}\frac{\partial^2 \tau}{\partial z \partial l} = -\frac{\partial w}{\partial x}. \tag{3}$$

Substituting the change in traveltime field shape due to source perturbation, $D_x = \frac{\partial \tau}{\partial l}$, into equation 3 provides a first order linear equation in D_x given by:

$$2\frac{\partial \tau}{\partial x}\frac{\partial D_x}{\partial x} + 2\frac{\partial \tau}{\partial y}\frac{\partial D_x}{\partial y} + 2\frac{\partial \tau}{\partial z}\frac{\partial D_x}{\partial z} = -\frac{\partial w}{\partial x}. \tag{4}$$

Solving for D_x requires the velocity (sloth) field as well as the traveltime field τ for a source located at the surface at l_0. Thus,the traveltime field for a source at l can be approximated by

$$t(x, y, z) \approx \tau(x, y, z) + D_x(x, y, z)(l - l_0). \tag{5}$$

Equation 4 is velocity dependent, which limits its use for inversion purposes. However, a differentiation of Equation 2 with respect to x produces

$$2\frac{\partial \tau}{\partial x}\frac{\partial^2 \tau}{\partial x^2}+2\frac{\partial \tau}{\partial y}\frac{\partial^2 \tau}{\partial x \partial y}+2\frac{\partial \tau}{\partial z}\frac{\partial^2 \tau}{\partial x \partial z}=\frac{\partial w}{\partial x}. \tag{6}$$

Adding equations 3 and 6 yields equation

$$\frac{\partial \tau}{\partial x}\frac{\partial^2 \tau}{\partial x \partial l}+\frac{\partial \tau}{\partial y}\frac{\partial^2 \tau}{\partial y \partial l}+\frac{\partial \tau}{\partial z}\frac{\partial^2 \tau}{\partial z \partial l}=\frac{\partial \tau}{\partial x}\frac{\partial^2 \tau}{\partial x^2}+\frac{\partial \tau}{\partial y}\frac{\partial^2 \tau}{\partial x \partial y}+\frac{\partial \tau}{\partial z}\frac{\partial^2 \tau}{\partial x \partial z}, \tag{7}$$

which is velocity independent. Substituting again the change in traveltime with source location $D_x = \frac{\partial \tau}{\partial l}$ into equation 7 yields

$$\frac{\partial \tau}{\partial x}\frac{\partial D_x}{\partial x}+\frac{\partial \tau}{\partial y}\frac{\partial D_x}{\partial y}+\frac{\partial \tau}{\partial z}\frac{\partial D_x}{\partial z}=\frac{\partial \tau}{\partial x}\frac{\partial^2 \tau}{\partial x^2}+\frac{\partial \tau}{\partial y}\frac{\partial^2 \tau}{\partial x \partial y}+\frac{\partial \tau}{\partial z}\frac{\partial^2 \tau}{\partial x \partial z}, \tag{8}$$

which is a first order linear partial differential equation in D_x with D_x=0 at the source. The traveltime derivatives are computed for a given traveltime field τ corresponding to a source location l_0. Equation 8 can be represented in a vector notation as follows:

$$\nabla \tau \cdot \nabla D_x \;=\; \nabla \tau \cdot \nabla \frac{\partial \tau}{\partial x}. \tag{9}$$

A similar treatment for a change of the source location in y or z yields the following equations, respectively:

$$\frac{\partial \tau}{\partial x}\frac{\partial D_y}{\partial x}+\frac{\partial \tau}{\partial y}\frac{\partial D_y}{\partial y}+\frac{\partial \tau}{\partial z}\frac{\partial D_y}{\partial z}=\frac{\partial \tau}{\partial x}\frac{\partial^2 \tau}{\partial x \partial y}+\frac{\partial \tau}{\partial y}\frac{\partial^2 \tau}{\partial y^2}+\frac{\partial \tau}{\partial z}\frac{\partial^2 \tau}{\partial y \partial z}, \tag{10}$$

or

$$\nabla \tau \cdot \nabla D_y \;=\; \nabla \tau \cdot \nabla \frac{\partial \tau}{\partial y}. \tag{11}$$

and

$$\frac{\partial \tau}{\partial x}\frac{\partial D_z}{\partial x}+\frac{\partial \tau}{\partial y}\frac{\partial D_z}{\partial y}+\frac{\partial \tau}{\partial z}\frac{\partial D_z}{\partial z}=\frac{\partial \tau}{\partial x}\frac{\partial^2 \tau}{\partial x \partial z}+\frac{\partial \tau}{\partial y}\frac{\partial^2 \tau}{\partial y \partial z}+\frac{\partial \tau}{\partial z}\frac{\partial^2 \tau}{\partial z^2}, \tag{12}$$

or

$$\nabla \tau \cdot \nabla D_z \;=\; \nabla \tau \cdot \nabla \frac{\partial \tau}{\partial z}. \tag{13}$$

The above set of equations provides a tool for calculating first-order traveltime derivatives with respect to the source location. However, a condition for stability is that the velocity field must be continuous. This condition is analogous to conditions used in ray tracing methods and can be enforced using smoothing techniques. Another approach to handle this limitation is discussed later.

A LINEAR VELOCITY MODEL EXAMPLE

As a first test to our formulations, we consider a 2-D model where the velocity changes linearly in the direction of the source perturbation. In this case, the traveltime is described analytically as a function of x and z and so will the traveltime changes, D_x. Restricting this example to models with change of velocity in the direction of the source perturbation does not limit its generality since changes in the orthogonal direction has no direct influence on the traveltime field.

In the first example, we consider a source perturbation in the vertical direction in a medium in which the velocity changes linearly in the vertical direction. Considering source perturbation in the vertical direction is useful for applications related to datuming and possibly downward continuation. The linear velocity model is defined by

$$v(z) = v_0 + az. \tag{14}$$

where a is the vertical velocity gradient and v_0 is velocity at the surface $z = 0$. The traveltime from a source at $x = z = 0$ to a point in the subsurface given by x and z is provided by Slotnick (1959), as follows:

$$\tau(x,z) = \frac{1}{a}\cosh^{-1}\left(\frac{a^2z^2\left(\frac{x^2}{z^2}+1\right)}{2v_0\left(az+v_0\right)}+1\right). \tag{15}$$

Evaluating $\frac{\partial\tau}{\partial x}$ and $\frac{\partial\tau}{\partial y}$ and using equation 4 yields:

$$D_z = -\frac{\left(az+2v_0\right)\sqrt{\frac{a^2(x^2+z^2)}{a^2x^2+(az+2v_0)^2}}}{v_0\left(az+v_0\right)}, \tag{16}$$

which is an analytical representation of the change in the traveltime field shape with source depth location for this specific linear model and can be used to predict the traveltime for a source at a different depth. To test equation 16, we use equation 15 to estimate the traveltime using expansion 5 and compare that with the true traveltime for that source. Figure 2 shows this difference for a model with (a) a vertical velocity gradient of 0.5 s^{-1} and (b) a vertical velocity gradient of 0.7 s^{-1}. A 200 meter vertical shift, used here for the source, is typical of corrections applied in datuming among other applications. The errors, as expected, increase with an increase in velocity gradient as zero velocity gradient results in no change in traveltime shape and thus no errors. However, the errors are generally small for both gradients with the maximum value of 0.007 s occurring for the largest offset to depth ratio.

In the second example, we consider source perturbation laterally in a medium in which the velocity changes linearly in the lateral direction. Considering source perturbation in the lateral direction could be useful for velocity estimation, beam based imaging, and interpolation applications, and more inline with the objectives of this study. In this case, the linear velocity model is defined by

$$v(x) = v_0 + ax. \tag{17}$$

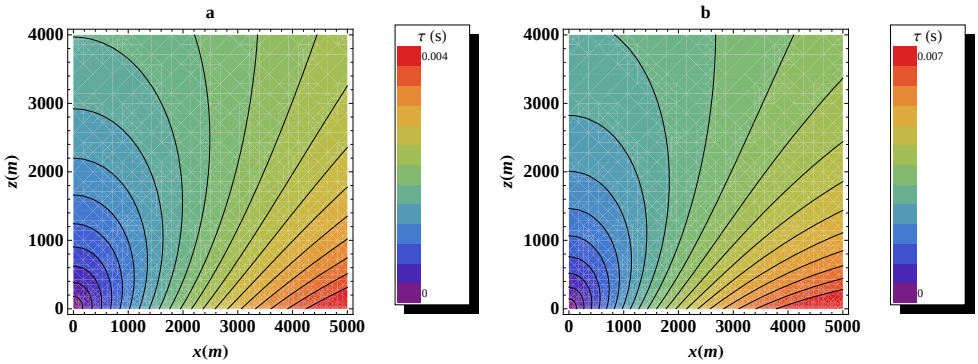

Figure 2: A color contour plot of the traveltime errors using the perturbation equation as a function of location (x, z) for a linear velocity model of with v_0=2000 m/s and a vertical velocity gradient of $0.5s^{-1}$ for (a) and $0.7s^{-1}$ for (b). In both cases, the vertical source perturbation distance is 200 meters. The maximum traveltime errors are (a) 0.004 s and (b) 0.007 s.

where a is now the lateral velocity gradient and v_0 is velocity at the vertical line $x = 0$. The traveltime and D_x are given by formulations similar to equations 15 and 16, but with an orthogonal transformation of coordinates. Though the equations are similar, we want to get an estimate of the error distribution for this problem. Figure 3 shows the traveltime errors for using these new formula to predict the changes due to shifts in the source location by (a) 100 meters and (b) 200 meters. As expected, the errors increase with the amount of shift. However, in both cases the errors are generally small and bounded by 0.002 s.

HIGHER-ORDER ACCURACY

The accuracy of the above formulations are first order in source perturbation, which is valid for small perturbation distances. To obtain a higher-order accuracy, we differentiate equation 3 again with respect to l yielding:

$$2\left(\frac{\partial^2\tau}{\partial x\partial l}\right)^2+2\frac{\partial\tau}{\partial x}\frac{\partial^3\tau}{\partial x\partial l^2}+2\left(\frac{\partial^2\tau}{\partial y\partial l}\right)^2+2\frac{\partial\tau}{\partial y}\frac{\partial^3\tau}{\partial y\partial l^2}+2\left(\frac{\partial^2\tau}{\partial z\partial l}\right)^2+2\frac{\partial\tau}{\partial z}\frac{\partial^3\tau}{\partial z\partial l^2}=\frac{\partial^2 w}{\partial x^2}. \tag{18}$$

Substituting the second derivative of traveltime with respect to source location $D_{xx} = \frac{\partial^2\tau}{\partial l^2}$ into equation 18 provides us with a first order linear partial differential

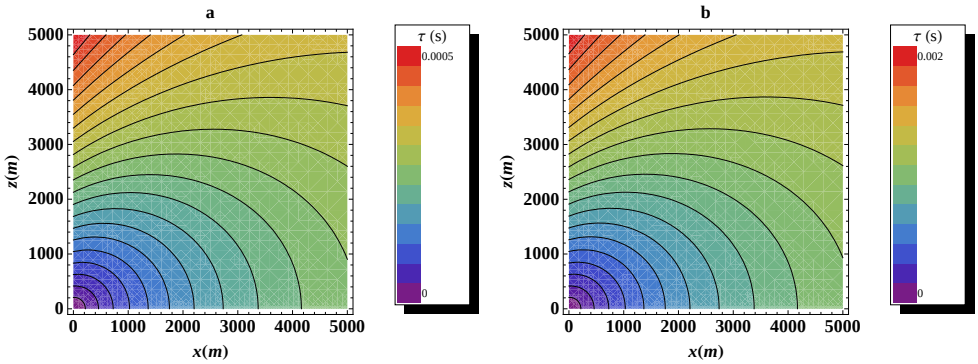

Figure 3: A color contour plot of the traveltime errors using the perturbation equation as a function of location (x, z) for a linear velocity model of with v_0=2000 m/s and a horizontal velocity gradient of $0.5s^{-1}$ for (a) a horizontal source perturbation of 100 meters and (b) a horizontal source perturbation distance of 200 meters. The maximum traveltime errors are (a) 0.0005 s and (b) 0.002 s.

equation in D_{xx} given by:

$$2\left(\frac{\partial D_x}{\partial x}\right)^2 + 2\frac{\partial \tau}{\partial x}\frac{\partial D_{xx}}{\partial x} + 2\left(\frac{\partial D_x}{\partial y}\right)^2 + 2\frac{\partial \tau}{\partial y}\frac{\partial D_{xx}}{\partial y} + 2\left(\frac{\partial D_x}{\partial z}\right)^2 + 2\frac{\partial \tau}{\partial z}\frac{\partial D_{xx}}{\partial z} = \frac{\partial^2 w}{\partial x^2}, \tag{19}$$

or

$$\nabla D_x \cdot \nabla D_x + \nabla \tau \cdot \nabla D_{xx} = \frac{1}{2}\frac{\partial^2 w}{\partial x^2} \tag{20}$$

This equation is similar in form to the first order equations, but with a different source function. Of course, D_x must be evaluated first using equation 4 to solve equation 20.

Based on Taylor's series expansion, the traveltime for a source at l is approximated by

$$t(x, y, z) \approx \tau(x, y, z) + D_x(x, y, z)(l - l_0) + \frac{1}{2}D_{xx}(x, y, z)(l - l_0)^2. \tag{21}$$

Using an infinite series representation by defining poles to eliminate the most pronounced transient behavior using Shanks transforms (Bender and Orszag, 1978), we can represent the second order Taylor's expansion in equation 21 as follows

$$t(x, y, z) \approx \tau(x, y, z) + \frac{{D_x}^2(x, y, z)(l - l_0)}{D_x(x, y, z)(l - l_0) + \frac{1}{2}D_{xx}(x, y, z)(l - l_0)^2}, \tag{22}$$

which can provide a better approximation results in some regions but has an obvious singularity that might cause divergence when the denominator tends to zero.

Similar equations for expansions in 3-D are obtained with the help of the following matrix

$$\begin{pmatrix} D_{xx} & D_{xy} & D_{xz} \\ D_{xy} & D_{yy} & D_{yz} \\ D_{xz} & D_{yz} & D_{zz} \end{pmatrix} = \begin{pmatrix} \frac{\partial^2 \tau}{\partial l_x^2} & \frac{\partial^2 \tau}{\partial l_x l_y} & \frac{\partial^2 \tau}{\partial l_x l_z} \\ \frac{\partial^2 \tau}{\partial l_x l_y} & \frac{\partial^2 \tau}{\partial l_y^2} & \frac{\partial^2 \tau}{\partial l_y l_z} \\ \frac{\partial^2 \tau}{\partial l_x l_z} & \frac{\partial^2 \tau}{\partial l_y l_z} & \frac{\partial^2 \tau}{\partial l_z^2} \end{pmatrix}, \tag{23}$$

with components obtainable using similar first order partial differential equations shown in Appendix A, where l_x, l_y, and l_z describe source perturbations in the x, y, and z directions, respectively. These equations can form the basis for beam expansions in beam-type migrations.

The higher-order equations provide better approximations of the traveltime perturbation. However, they require both the velocity and its derivative to be continuous in the direction of the source perturbation.

ALGORITHM

All the traveltime source perturbation equations developed above are linear first order partial differential equations that can be solved using any of the many upwind numerical methods. Similar to Franklin and Harris (2001) and Alkhalifah (2002), we will rely on the fast marching method Sethian (1996) to solve such linear equations.

An update procedure for such a method is based on an upwind first or second-order approximation to the new equations. In simple terms, the procedure starts with selecting one or more (up to three) neighboring points around the updated point. The traveltime values at the selected neighboring points need to be smaller than the current value. After the selection, one solves the discrete version of the linear partial differential equation for D_x. We add this perturbation value multiplied by the perturbation distance to the background traveltime. As the result of the updating, either a *FarAway* point is marked as *NarrowBand* or a *NarrowBand* point gets assigned a new value. This process is repeated until we run out of points in the narrow band.

In all cases, we will need the traveltime field for a given source obtained using the eikonal equation or ray-based methods. This traveltime field serves as the background field for predicting the traveltime for other sources. For the first-order accuracy expansion, we have to only solve the linear source differential eikonal partial differential equation once. However, for the second order expansion or its shank transform representation, we will need D_{xx}, and thus need to solve an equivalent linear differential equation again.

The critical part of solving these equations is the need to evaluate the first and second order derivatives of the velocity field or equivalently the second- and third-order derivatives of the background traveltime field all with respect to the direction in which the source is perturbed. This poses a challenge in media where the velocity

changes abruptly in that direction. Therefore, some smoothing may be required for the velocity field in the source perturbation direction.

EXAMPLES

Lens example

Since the differential equation depends on velocity changes in the direction of the source shift, we test the methodology on a model that contains a lens anomaly in an otherwise constant velocity gradient ($\frac{dv}{dx} = 0.5s^{-1}$ and $\frac{dv}{dz} = 0.7s^{-1}$ with velocity at the origin equal to 2 km/s) model. The lens is located at 600 meters laterally and 500 meters depth with a velocity perturbation of +500 m/s (or 20%). The lens has a diameter of 200 meters and causes a large velocity variation. Using this model, we test the accuracy of the first-order, second-order, and the Shanks-transform representation equations.

For a source located at 200 meters lateral distance from origin and 200 meter depth, we solve the eikonal equation using the fast marching method with second order accuracy. The traveltime field in this case is represented by the solid contours on the left side plots of Figures 4, 5, and 6. We also solve the eikonal equation for source located virtually 100 meters away in lateral direction and it is represented by the solid curves in the middle plot of the three Figures. Solving for D_x using equation 3 and using that along with the original traveltime field, we obtain an approximate traveltime field for a source 100 meters away. This new traveltime field is represented by the dashed contour curves in Figure 4. The absolute difference between the simulated traveltime and the true one both displayed in the center plot is given by the density plot shown on the right side of Figure 4.

The errors are generally small (less than 0.008 s), with the largest of errors appearing on the lower side of the lens. This error is generally small considering the large shift (100 meters) and first-order nature of the expansion. In addition, errors for the rest of the traveltime field corresponding to the linear variation in velocity is extremely small.

Figure 5 is similar to Figure 4, but now we use the second-order expansion, which requires solving the linear partial differential equation twice. Overall, as expected, the errors are less than the first order case with clear reduction in the upper side trail of the lens.

With hardly any additional computational cost, we can use the Shank transform representation of the expansion and in this case the errors, as shown in Figure 6, are reduced even further.

To emphasize the role of the perturbation terms in approximating the source-

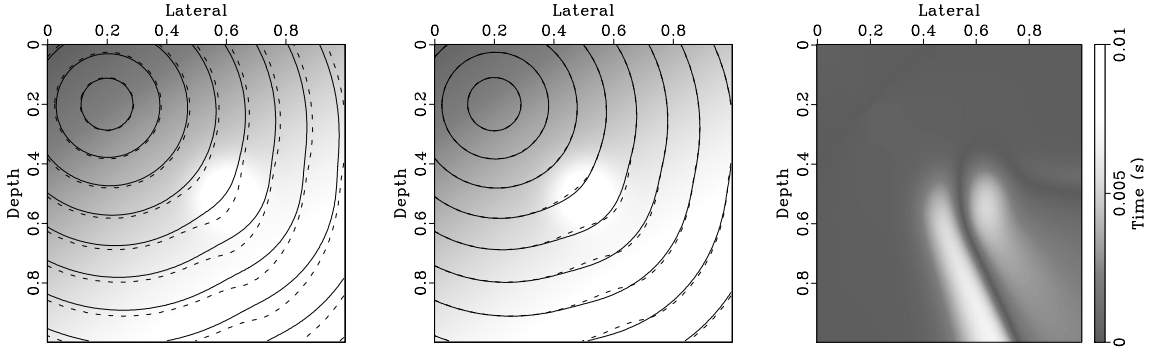

Figure 4: The traveltime contour (solid curve) plot for a source at lateral and depth position of 0.2 km (left) and for a source virtually perturbed by 100 meters in the lateral direction (middle), both compared with the traveltime derived using the first-order accuracy perturbation eikonal for a 100 meters virtual shift (dashed curves). In both plots the velocity field is shown in the background. Also shown on the right is a density plot of the difference between the two contours in the middle plot.

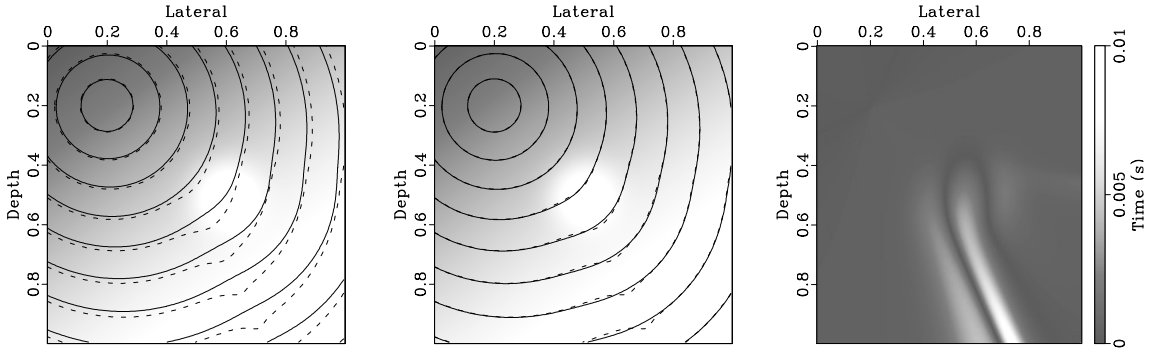

Figure 5: The traveltime contour (solid curve) plot for the original source (left) and for a source virtually perturbed by 100 meters in the lateral (middle), both compared with the traveltime derived using the second-order accuracy perturbation eikonal for a 100 meters virtual shift (dashed curves). In both plots the velocity field is shown in the background. Also shown on the right is a density plot of the difference between the two contours in the middle plot.

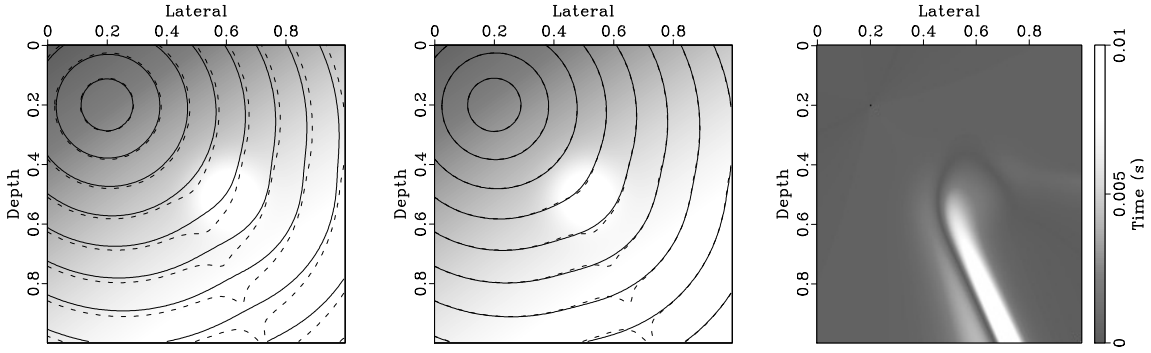

Figure 6: The traveltime contour (solid curve) plot for the original source (left) and for a source virtually perturbed by 100 meters (middle), both compared with the traveltime derived using Shanks transform perturbation eikonal for a 100 meters virtual shift (dashed curves). In both plots the velocity field is shown in the background. Also shown on the right is a density plot of the difference between the two contours in the middle plot.

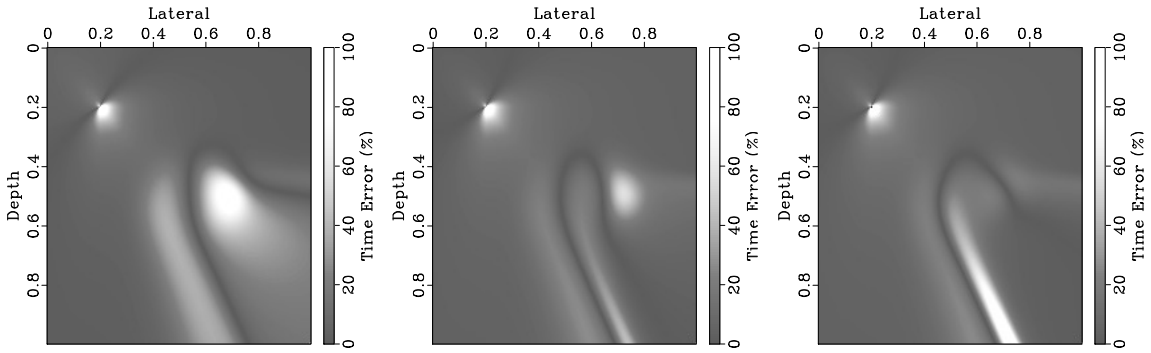

Figure 7: A density plot of the traveltime error in percent for the difference plots in Figures 4-6 (right), plotted from left to right, respectively. The percent error is measured in a relative manner where 0 corresponds to the accurate traveltime and 100% to the unperturbed traveltime.

shifted traveltime, we define a relative percent error as

$$t_{err} = 100\frac{\tau - \tau_0}{\tau_1 - \tau_0}, \tag{24}$$

where τ_0 is the unperturbed traveltime for the original source, τ_1 is the traveltime for the desired source calculated directly using the conventional eikonal equation, and τ is the traveltime estimated using the perturbation equations for the desired source. If τ is equal to τ_1, as desired, the error is zero. However, if τ equals the unperturbed traveltime τ_0 the error is 100 percent. Figure 7 shows this relative errors for the first-order accuracy perturbation (left), the second-order accuracy perturbation (middle), and using Shanks transform perturbation (right) for the linear model with a lens. The errors are overall less for the Shanks transform perturbation. The large error at position and depth equal to 0.2 km corresponds to the source location, where the denominator of equation 24 tends to zero.

Marmousi example

Despite the fact that the source perturbation differential equations are dependent on the derivative of velocity, and thus, discontinuous velocity fields pose a problem, we test the method on the unsmoothed Marmousi model (Versteeg, 1994) to asses the stability of the numerical process. In this case, we use only the first order expansion to avoid relying on higher order derivatives of the velocity field, which might breakdown here.

Figure 8 shows the Marmousi model in the background with the traveltime field contours computed directly using the finite difference eikonal equation for a source located at 4.2 km at the surface (dashed curves) compared with the traveltime field perturbed from a source located 200 meters away at 4 km surface location. The two contour curves overlap near the source, but show some difference away from the source. However, the difference is generally small considering the large source perturbation of 200 meters and the velocity complex model.

A closer and more quantitative look is given by the difference plot; Figure 9 shows a density plot for the difference in traveltime contours in Figure 8. With a clip of 0.01 seconds, errors given in gray are small and dominate the plot. This is a testament to the stability of the Fast marching implementation despite the complex velocity field that includes many lateral discontinuities.

DISCUSSION

Seismic data are usually acquired with geophone layouts that record information from multiple source locations. The redundancy in the coverage is necessary to eliminate gaps in the data, estimate velocity, and image the data. Thus, the direct relation

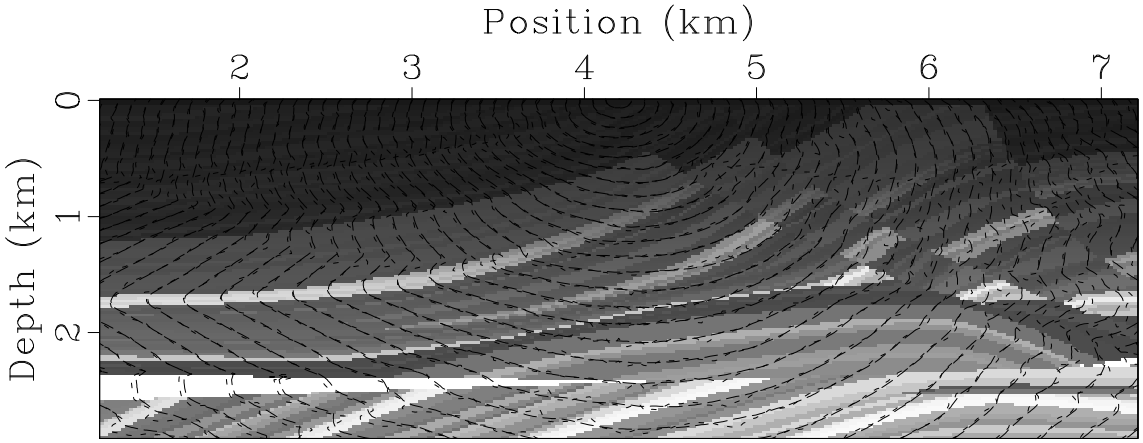

Figure 8: The traveltime contour plot for a source at the surface at 4.2 km (dashed curves) and for a source virtually perturbed by 200 meters from the traveltime field at 4 km source surface location (solid curves). The perturbed traveltime is derived using the first-order accuracy perturbation eikonal. The Marmousi velocity field is shown in the background.

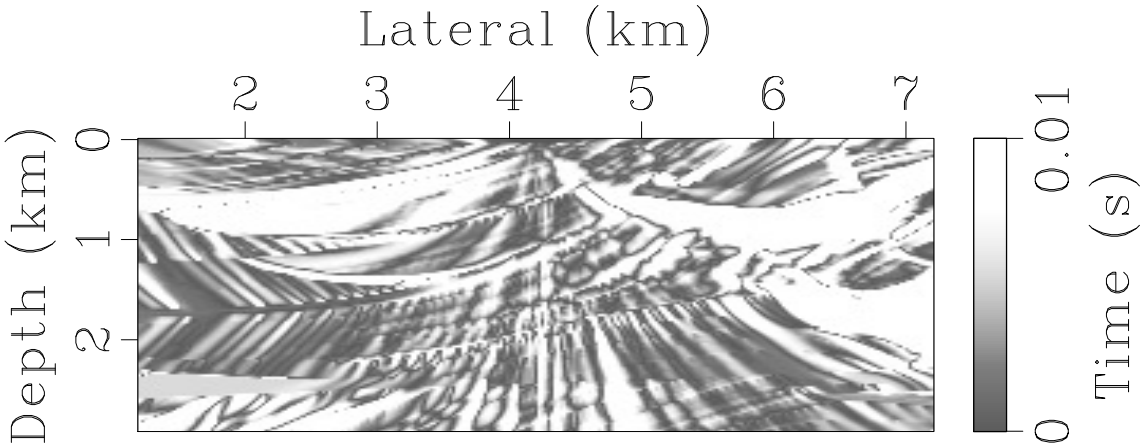

Figure 9: A density plot for the difference between the two contours shown in Figure 8.

between the traveltime field and the source location allows us to estimate attributes that can help in interpolation, velocity estimation and possibly imaging. Specifically:

- Traveltime compression schemes (Alkhalifah, 2010) require the ability to interpolate subsampled traveltimes.
- One of the main sources of trace interpolation information is the behavior of wavefronts with respect to the source location.
- Velocity estimation relies directly on the change in traces as a function of source and receiver locations.
- Kirchhoff antialiasing schemes (Lumley et al., 1994; Abma et al., 1999) explicitly require the derivatives of the traveltime with respect to the source and receiver locations on the surface.
- Gaussian-beam migration (Hill, 1990, 2001; Alkhalifah, 1995; Gray, 2005) relies on traveltime derivative information as a function of ray angle variations and source variations, which is usually obtained from the slower and less stable dynamic ray tracing.
- Efficient traveltime calculation can be achieved using first order linear equations instead of the nonlinear form of the eikonal equation.

However, the formulation developed here has limitations. Chief among them is the need to evaluate derivatives of velocity and traveltime fields. Since velocities may include discontinuities, their derivatives are not easy to evaluate. However, similar to the ray-based methods, one can simply smooth the velocity field.

Since traveltime fields that contain all arrivals satisfy the eikonal equation, the source perturbation can be applied to traveltimes extracted from other methods, such as ray tracing or escape equations. Therefore, they can include most energetic arrivals as opposed to first-arrival traveltimes.

CONCLUSIONS

The behavior of the traveltime field shape as a function of source location in an inhomogeneous medium provides a platform for many useful applications. We present eikonal-based equations that relate traveltime field changes with respect to the source perturbations. These equations are linear first-order differential equations that depend on the background traveltime and velocity fields. Their solutions describe the first- and second-order changes in the traveltime field as a function of the source location. These equations are equivalent to the plane wave expansion extracted from dynamic ray tracing, such as the one used for Gaussian-beam migration. They can be solved efficiently by finite-difference solvers on a regular grid. The solutions are used to estimate the traveltime shape for neighboring sources. The accuracy of the

equations depends on the complexity of lateral velocity variations as well as on the source perturbation distance.

ACKNOWLEDGMENTS

The first author thanks KACST and KAUST for their support of this research. We thank the editors and the reviewers of Geophysics for their critical review of the paper and the resulting improvements.

REFERENCES

Abma, R., J. Sun, and N. Bernitsas, 1999, Antialiasing methods in Kirchhoff migration: Geophysics, **64**, 1783–1792.

Aldridge, D. F., 1994, Linearization of the eikonal equation (short note): Geophysics, **59**, 1631–1632.

Alkhalifah, T., 1995, Gaussian beam depth migration for anisotropic media: Geophysics, **60**, 1474–1484.

———, 2002, Traveltime computation with the linearized eikonal equation for anisotropic media: Geophys. Prosp., **50**, 373–382.

———, 2010, Efficient traveltime compression for 3D prestack kirchhoff migration: Geophysical Prospecting, in print, **58**.

Alkhalifah, T., and S. Fomel, 2001, Implementing the fast marching eikonal solver: spherical versus Cartesian coordinates: Geophys. Prosp., **49**, 165–178.

Bender, C. M., and S. A. Orszag, 1978, Advanced mathematical methods for scientists and engineers: McGraw-Hill.

Bevc, D., 1997, Imaging complex structures with semirecursive Kirchhoff migration: Geophysics, **62**, 577–588.

Fomel, S., and J. A. Sethian, 2002, Fast phase-space computation of multiple arrivals: Proceedings of the National Academy of Sciences, **99**, 7329–7334.

Franklin, J. B., and J. M. Harris, 2001, A high-order fast marching scheme for the linearized eikonal equation: Journal of Computational Acoustics, **9**, 1095–1109.

Geoltrain, S., and J. Brac, 1993, Can we image complex structures with first-arrival traveltime?: Geophysics, **58**, 564–575.

Gray, S. H., 2005, Gaussian beam migration of common-shot records: Geophysics, **70**, S71–S77.

Hill, N. R., 1990, Gaussian beam migration: Geophysics, **55**, 1416–1428.

———, 2001, Prestack Gaussian-beam depth migration: Geophysics, **66**, 1240–1250.

Kim, S., 2002, 3-D eikonal solvers: First-arrival traveltimes: Geophysics, **67**, 1225–1231.

Lumley, D. E., J. F. Claerbout, and D. Bevc, 1994, Anti-aliased Kirchhoff 3-D migration: 64th Ann. Internat. Mtg, Soc. of Expl. Geophys., 1282–1285.

Podvin, P., and I. Lecomte, 1991, Finite difference computation of traveltimes in very

contrasted velocity models: A massively parallel approach and its associated tools: Geophysical Journal International, **105**, 271–284.
Popovici, A. M., and J. Sethian, 2002, 3-D imaging using higher order fast marching traveltimes: Geophysics, **67**, 604–609.
Qian, J., and W. W. Symes, 2002, An adaptive finite-difference method for traveltimes and amplitudes: Geophysics, **67**, 167–176.
Sethian, J. A., 1996, A fast marching level set method for monotonically advancing fronts: Proc. Nat. Acad. Sci., **93**, 1591–1595.
Sethian, J. A., and A. M. Popovici, 1999, 3-D traveltime computation using the fast marching method: Geophysics, **64**, 516–523.
Slotnick, M. M., 1959, Lessons in Seismic Computing: Soc. of Expl. Geophys. (Edited by R. A. Geyer).
Symes, W. W., and J. Qian, 2003, A slowness matching Eulerian method for multivalued solutions of eikonal equations: Journal of Scientific Computing, **19**, 501–526.
van Trier, J., and W. W. Symes, 1991, Upwind finite-difference calculation of traveltimes: Geophysics, **56**, 812–821.
Versteeg, R., 1994, The Marmousi experience: Velocity model determination on a synthetic complex data set: The Leading Edge, **13**, 927–936.
Vidale, J. E., 1988, Finite-difference calculation of traveltimes: Bull. Seis. Soc. Am., **6**, 20622076.
———, 1990, Finite-difference calculation of traveltimes in three dimensions: Geophysics, **55**, 521–526.
Zhao, H.-K., 2005, A fast sweeping method for eikonal equations: Mathematics of Computation, **74**, 603–627.

APPENDIX A: HIGHER-ORDER EXPANSIONS

Traveltime behavior due to source perturbations can be estimated more accurately using higher-order formulations. Considering that l_x, l_y, and l_z represent source perturbations in the x, y, and z directions, respectively, a full representation of the second derivative behavior is given by the following symmetric matrix

$$\begin{pmatrix} D_{xx} & D_{xy} & D_{xz} \\ D_{xy} & D_{yy} & D_{yz} \\ D_{xz} & D_{yz} & D_{zz} \end{pmatrix} = \begin{pmatrix} \frac{\partial^2 \tau}{\partial l_x^2} & \frac{\partial^2 \tau}{\partial l_x l_y} & \frac{\partial^2 \tau}{\partial l_x l_z} \\ \frac{\partial^2 \tau}{\partial l_x l_y} & \frac{\partial^2 \tau}{\partial l_y^2} & \frac{\partial^2 \tau}{\partial l_y l_z} \\ \frac{\partial^2 \tau}{\partial l_x l_z} & \frac{\partial^2 \tau}{\partial l_y l_z} & \frac{\partial^2 \tau}{\partial l_z^2} \end{pmatrix}. \tag{A-1}$$

D_{xx} is evaluated using the first order linear differential equation 20, where τ is obtained from solving the eikonal equation and D_x is evaluated from equation 4.

Similarly, higher order approximations in l_y and l_z are given by

$$\nabla D_y \cdot \nabla D_y + \nabla \tau \cdot \nabla D_{yy} = \frac{1}{2} \frac{\partial^2 w}{\partial y^2} \tag{A-2}$$

and

$$\nabla D_z \cdot \nabla D_z + \nabla \tau \cdot \nabla D_{zz} = \frac{1}{2}\frac{\partial^2 w}{\partial z^2}, \tag{A-3}$$

respectively, which represent the diagonal terms of the matrix in equation A-1.

To obtain the non-diagonal components of the matrix we differentiate equation 3 with respect to l_y, instead of l_x, yielding:

$$2\left(\frac{\partial^2 \tau}{\partial x \partial l_x}\right)\left(\frac{\partial^2 \tau}{\partial x \partial l_y}\right) + 2\frac{\partial \tau}{\partial x}\frac{\partial^3 \tau}{\partial x \partial l_x \partial l_y} + 2\left(\frac{\partial^2 \tau}{\partial y \partial l_x}\right)\left(\frac{\partial^2 \tau}{\partial y \partial l_y}\right) + 2\frac{\partial \tau}{\partial y}\frac{\partial^3 \tau}{\partial y \partial l_x \partial l_y} + 2\left(\frac{\partial^2 \tau}{\partial z \partial l_x}\right)\left(\frac{\partial^2 \tau}{\partial z \partial l_y}\right) + 2\frac{\partial \tau}{\partial z}\frac{\partial^3 \tau}{\partial z \partial l_x \partial l_y} = \frac{\partial^2 w}{\partial x \partial y}. \tag{A-4}$$

Substituting the second derivative of traveltime with respect to source location $D_{xy} = \frac{\partial^2 \tau}{\partial l_x \partial l_y}$ into equation A-4 provides us with a first order linear equation in D_{xy} given by:

$$2\left(\frac{\partial D_x}{\partial x}\right)\left(\frac{\partial D_y}{\partial x}\right) + 2\frac{\partial \tau}{\partial x}\frac{\partial D_{xy}}{\partial x} + 2\left(\frac{\partial D_x}{\partial y}\right)\left(\frac{\partial D_y}{\partial y}\right) + 2\frac{\partial \tau}{\partial y}\frac{\partial D_{xy}}{\partial y} + 2\left(\frac{\partial D_x}{\partial z}\right)\left(\frac{\partial D_y}{\partial z}\right) + 2\frac{\partial \tau}{\partial z}\frac{\partial D_{xy}}{\partial z} = \frac{\partial^2 w}{\partial x \partial y}. \tag{A-5}$$

or

$$\nabla D_x \cdot \nabla D_y + \nabla \tau \cdot \nabla D_{xy} = \frac{1}{2}\frac{\partial^2 w}{\partial x \partial y}. \tag{A-6}$$

Similar equations for the rest of the matrix components are given by

$$\nabla D_x \cdot \nabla D_z + \nabla \tau \cdot \nabla D_{xz} = \frac{1}{2}\frac{\partial^2 w}{\partial x \partial z}, \tag{A-7}$$

and

$$\nabla D_y \cdot \nabla D_z + \nabla \tau \cdot \nabla D_{yz} = \frac{1}{2}\frac{\partial^2 w}{\partial y \partial z}, \tag{A-8}$$